Evaluation of Inverted Microstrip Gap Waveguide Bandpass Filters
for Ka-band

Nelson Castro[a], Francisco Pizarro[a,<], Luis Fernando Herrán-Ontanón[b] and Eva Rajo-Iglesias[c]

[a]Pontificia Universidad Católica de Valparaíso, Escuela de Ingeniería Eléctrica, Valparaíso, Chile
[b]Universidad de Oviedo, Oviedo, Spain
[c]Department of Communications and Signal Theory, Universidad Carlos III de Madrid, 28911 Madrid, Spain

ABS T RAC T

This article presents the implementation of three inverted microstrip gap-waveguide (IM-GWG) bandpass filters for theKa-band, at a central frequency of 28 GHz. This technology is a good candidate for the future communication systems operating in the millimeter-wave frequency bands due to the low loss characteristic and the easy manufacturing due to the increased size for these frequency bands. Three different topologies will be analyzed and their sensitivity to the position with respect to the pins of the bed of nails will be studied. Measurements confirm the good performance of the technology in terms of transmission and reflection coefficients over the whole assessed band.

1. Introduction

An important requirement for the new generation of communication systems is the increasing bandwidth demand, which implies that these systems will operate in frequency bands located in the upper part of the spectrum compared to the systems that are used nowadays [1, 2]. The migration to this part of the spectrum, namely millimeter waves (mm-waves), posses new issues for the design of the components of the communication systems. One issue is directly related to the dimensions of the devices, for example in printed technologies as microstrip lines, the overall size and parameters are directly related to the wavelength in use [3]. This reduction in the wavelength will have as consequence the implementation of very small printed circuit lines and overall dimensions that will be either difficult or expensive to manufacture. In addition, the substrates used as supporting structures for the printed circuits tend to have an increase in their losses when moving up in frequencies [4].

One technology candidate to overcome the losses introduced by the dielectric substrate and the manufacture issues is the inverted microstrip technology [5]. This technology consists of a microstrip line etched on a substrate, and over this line, separated by an air gap, is placed a conductive top lid. This configuration allows the propagation of a quasi-TEM mode in the air gap between the microstrip line and the top-lid, leading to a reduction of the losses, as the field is propagating mainly in the air, and to a reduction of the effective permittivity. This reduction of the effective permittivity impacts on the dimensions of the microstrip lines, so that for a given impedance value, the dimensions of the microstrip line will be larger, overcoming possible manufacturing issues. However, this technology has an important issue to be solved: as-is, a part of the electromagnetic energy leaks from the line, and therefore, exhibits radiation losses reducing the efficiency of the topology. One solution that can solve this problem is the use of metasurfaces by introducing a perfect magnetic conductor (PMC) boundary condition provided by a metasurface that in combination with the top lip of the inverted microstrip, will generate a stop-band at the desired frequency band. This imply that the electromagnetic wave will propagate only where the boundary conditions allow it (i.e., between the metal line and the top-lid). This technology is known as inverted microstrip gap waveguide (IM-GWG)[6], and has led to several implementations with the aim of reducing losses and packaging in mm-wave components [7, 8, 9, 10, 11]. The same concept can be also usedto provide the packaging to standard microstrip technology [12], obtaining a clear improvement in the performance of

the components but without solving the problem of the dielectric losses.

One important component in any communication system is the bandpass filter. For high frequency circuits and due to its good integration characteristics, these filters are usually made in microstrip technology. However, the increase of the operational frequency can led to the previously described issues for this component. On that scope, this work presents the design of three different inverted microstrip gap waveguide (IM-GWG) filters with a central frequency of 28 GHz that is a candidate frequency for the future generation of 5G wireless communications networks [13]. The article is divided as follows: Section 2 describes the design of the metasurface, in Section 3 the IM-GWG filters are designed and simulated, and in Section 4 the obtained measurement results are presented.
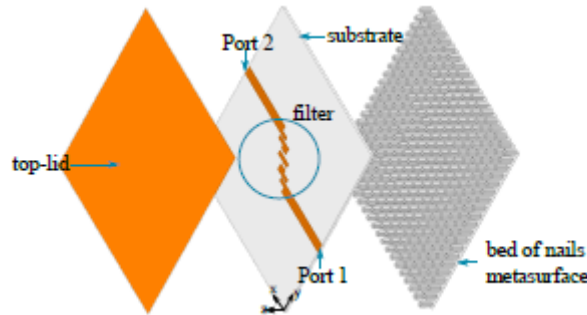
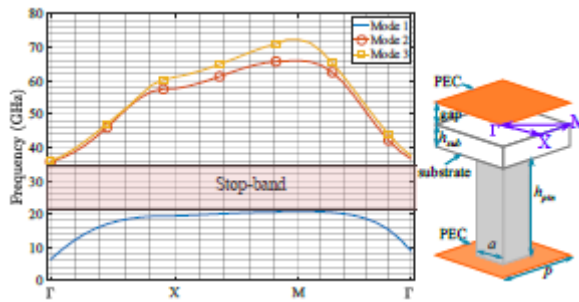

Figure 1: Exploded-view of the IM-GWG filter topology.

Figure 2: Dispersion diagram of the metasurface unit cell

2. Metasurface design

Fig. 1 shows an exploded-viewof the IM-GWGfilter configuration. The metasurface consists of a periodic structure made by conductive pins or bed of nails (BoN), which generates the boundary conditions of a PMC and therefore a stop-band on the operational frequency of the filter [14, 15]. On top of the BoN is placed a dielectric substrate withthe microstrip bandpass filter etched on top, along with the 50 microstrip feeding lines. Finally, on top of the etched substrate, it is placed a conductive top-lid, separated by an air gap.

The first step for the design of the filters is the design of the metasurface that generates the stop-band in the desiredfrequency band. To this aim, we evaluate the dispersion diagram generated by a unit-cell in the irreducible Brillouinzone. The proposed unit cell and the generated dispersion diagram are shown in Fig. 2. There are many constitutiveparameters that have an influence on the generation of the stop band [16], however, this design will be focused ongenerating a stop-band where the operational frequency of 28 GHz will be approximately at the center of it, in order toavoid any effect generated by the lower or upper limits of the stop-band [17]. The designed unit cell of periodicity p =2.05 mm consists of a conductive pin of lateral

dimensions a = 0.8 mm and a height hpin = 1.25 mm. On top of theconductive pin is placed a substrate with a relative permittivity of "r = 3 and height hsub = 0.5 mm. Over the substrate,separated by an air gap of 0.5 mm, is placed a perfect conductor (PEC) top plate. To have a parallel plate condition for the unit cell, a PEC plate is also placed at the bottom of the conductive pin. We can see from the dispersion diagram generated by the unit cell in Fig 2 that there is a stop-band occurring between 20.9 and 35.7 GHz, which includes the desired center frequency of the bandpass filters (28 GHz).

Once the metasurface structure is designed, we need to fix some dimensions of the filters that will be designed and constructed. For an easy integration in manufacture, all three filters will be etched using the same substrate, with thesame dimensions, in order to construct only one BoN structure. To this aim, a ROGERS R3003 is used, with a relative permittivity of "r = 3, and a loss tangent of tan = 0.0013. The lateral dimensions of the substrate are Ws= 33.2 mm, ls = 40 mm and a height of hsub = 0.5 mm. The gap between the substrate and the top-lid is of 0.5 mm, giving a microstrip line of width Wl = 1.9 mm to obtain 50 impedance for the feeding lines. In Fig. 3 a description of the common structure of the three filters to be designed is presented.
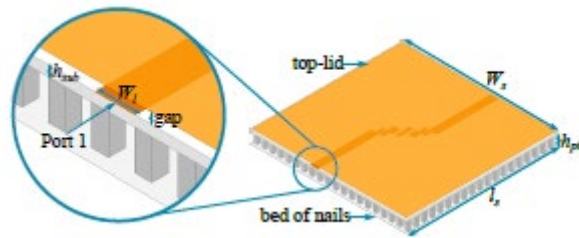

Figure 3: Shared dimensions of the designed IM-GWG filters.
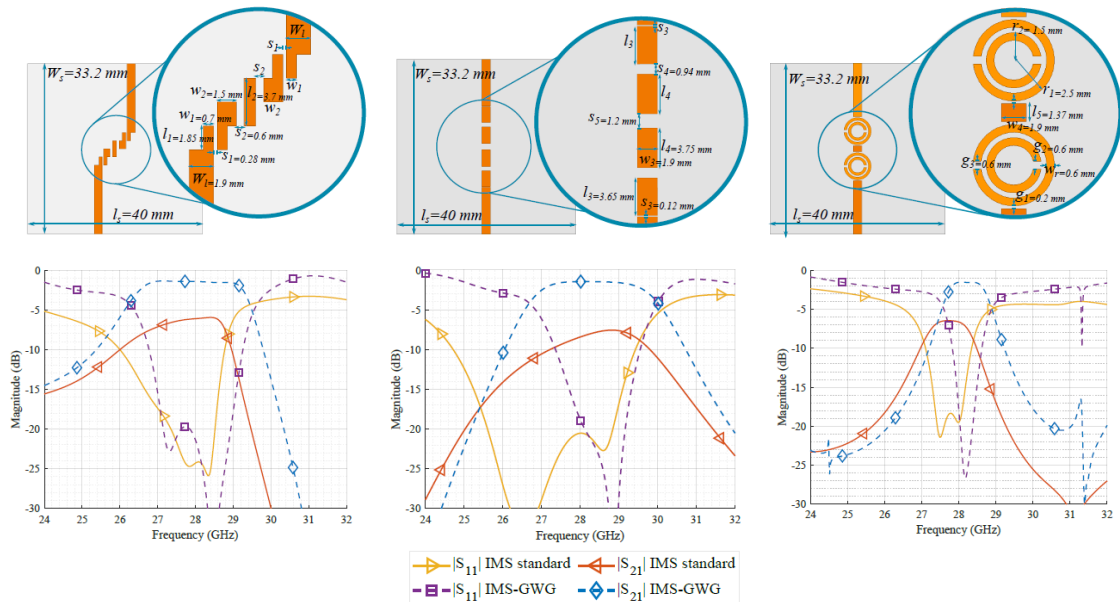

Figure 4: Top: Dimensions of the three designed IM-GWG filters, from left to right: parallel coupled lines filter, end-coupled lines filter and split-ring resonator filter. Bottom: transmission and reflection coefficients for each designed IM-GWG filter,compared to the same structure without metasurface, from left to right: parallel coupled lines filter, end-coupled lines filter and split-ring resonator filter.

3. Bandpass filter design

Once the common dimensions are set, we will design three different bandpass filter topologies to be assessed, namely parallel-coupled line filter, end-coupled line filter and split-ring resonator filter. All structures will be designed to operate with a central frequency of 28 GHz, then simulated using a full-wave simulation software HFSS [18], and compared to its same version, using the same dimensions, but without the metasurface, i.e. a standard inverted microstrip line. There is a first step in the design of the filters that consists of designing the filters using a PMC instead of the bed of nails [5, 10]. The resulting filter is then used as an initial version that is optimized replacing the PMC by the bed of nails.

In Fig. 4 the three different filters with their corresponding dimensions are shown. The first filter (top-left) is a 3rd order parallel-coupled lines one. The final dimensions of this filter are $l1 = 1.85$ mm, $w1 = 0.7$ mm, $s1 = 0.28$ mm, $s2 = 0.6$ mm, $l2 = 3.7$ mm and $w2 = 1.5$ mm. The second filter (top-middle) is a 4th order end-coupled line filter, with the following final dimensions: $s3 = 0.12$ mm, $l3 = 3.65$ mm, $w3 = 1.9$ mm, $l4 = 3.75$ mm, $s4 = 0.94$ mm and $s5 = 1.2$ mm. Finally, the 2nd order split-ring resonator filter (top-right) has the following dimensions: $g1 = 0.2$ mm, $g2 = 0.6$ mm, $g3 = 0.6$ mm, $w4 = 1.9$ mm, $wr = 0.6$ mm, $l5 = 1.37$ mm, $r1 = 2.5$ mm and $r2 = 1.5$ mm. To notice that all three topologies are commonly used in communication technologies.

The simulated transmission and reflection coefficients of the three designed filters, with and without the BoN metasurface are shown in Fig. 4 (bottom). We can see that for the three filter configurations (parallel-coupled, endcoupled and SRR from left to right), when the metasurface is not present, they have very poor performance in terms of their transmission coefficient in the band of interest. Even if the three configurations are well matched exhibiting low reflection coefficients in the band of interest, none of the filters has a transmission coefficient higher than -6 dB, which makes them unsuitable for any application. However, by applying the BoN required in IM-GWG technology, we can see that the transmission coefficients for the three designed filters exhibit a high transmission coefficient (above -2 dB) while keeping a good matching in the whole band of interest.

In order to verify the effect of the metasurface in the inverted microstrip filters, Fig. 5 contains a representation of the simulated electric fields in the air gap at 28 GHz, for the three filter structures (parallel-coupled, end-coupled and SRR, from left to right) without the metasurface (top) and with the metasurface (bottom). We can see that when the metasurface is not present, there is a significant part of the electric field that is not confined in the volume between the line and the top plate. On the other hand, and as expected, when the metasurface is applied, the stop-band generated does not allow the electric field to propagate outside the transmission line due to the imposed boundary conditions.This confirms the improvement in their transmission characteristics.

Now, the sensitivity of the three filters as a function of the change in their relative position with respect to the pins of the BoN is analyzed. It is known that in this version of the gap waveguide technology, the impedance of the line is affected by the relative position of the line with respect to the pins [17]. For this reason it is of interest to evaluate if among the three selected topologies for bandpass filters, there are differences in the sensitivity with this aspect. Two cases are simulated.

The cases under study are described in Figure 6, which are two extreme cases regarding the position of the input of the filter with respect to the BoN (the input line on top of the pins and the input line in between two pins). The resultsof the simulations are shown in Fig. 7. In these

figures we can see how the filter made with parallel couple lines is the one that is more affected by this change in the position whilst the split ring resonator geometry is almost unaffected by this change. It is important to remember that this is an important aspect as in practice, the position of the lines of any circuit with respect to the pins is rarely taken into account on the design of these structures.
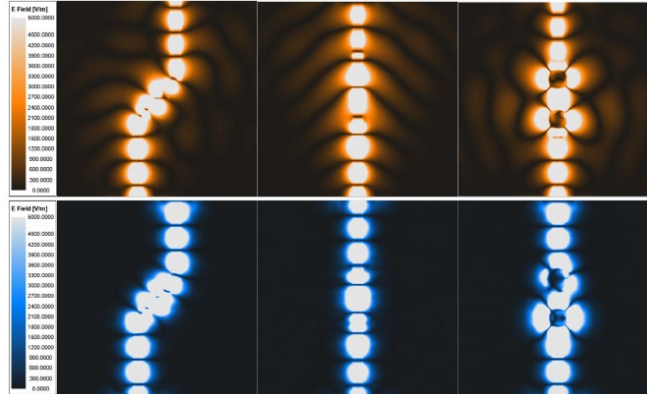

Figure 5: Simulated electric fields at 28 GHz for the three filter topologies. Top: without metasurface. Bottom: with metasurface.
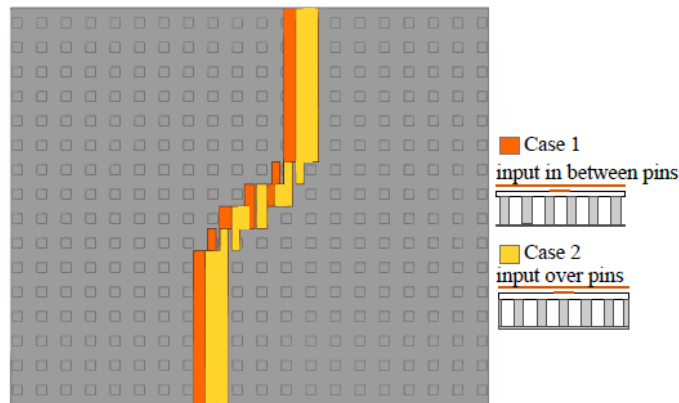

Figure 6: Study cases for sensitivity analysis regarding the position of the input of the IM-GWG with respect to the pins of the BoN.
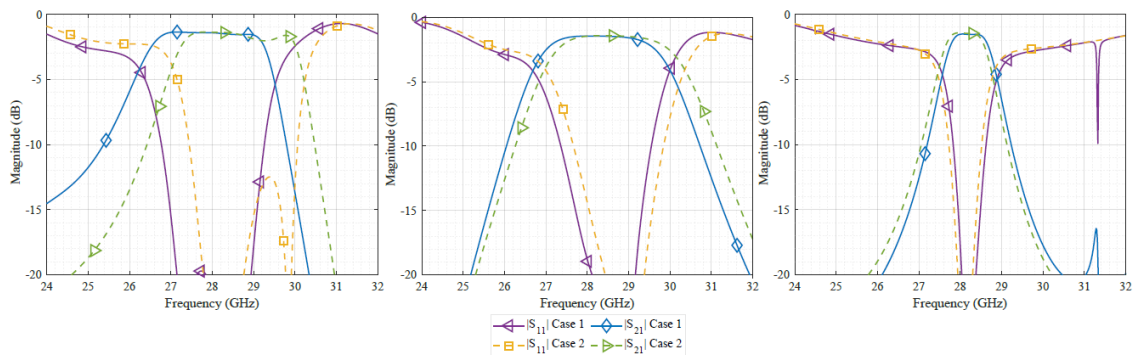

Figure 7: Comparison of the performance of the three filters as a function of the position of the lines w.r.t the pins. From left to right: parallel coupled lines filter, end-coupled lines filter and split-ring resonator filter.
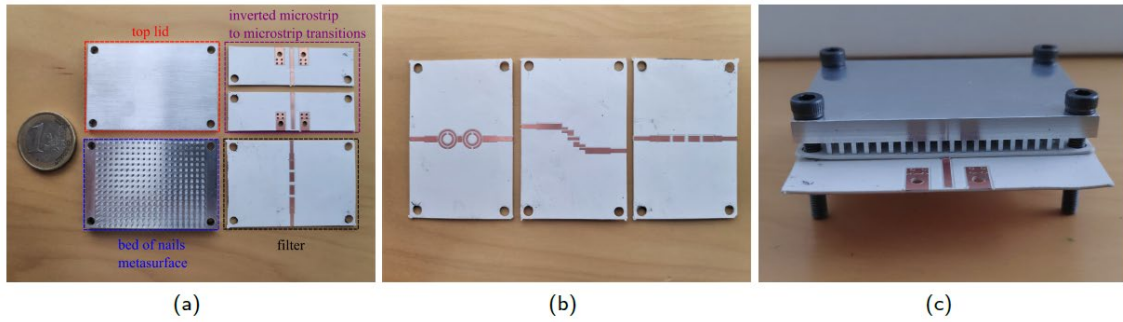
Figure 8: Constructed IM-GWG filters. a) IM-GWG constructed components. b) Top-view of the three constructed filters (from left to right: split ring resonator, parallel-coupled lines, end-coupled lines). c) Assembled IM-GWG filter with transitions.

4. Measurement results

Once the designed filters are validated by simulation, we proceed to the manufacture of the three structures. Fig. 8 shows the IM-GWG constructed filters, where we can identify different pieces of the designed filters. For this construction, the top lid and the bed of nails metasurface are both made with aluminium and the filter circuits are etched on a RO3003 substrate of height $hsub = 0.5$ mm with the same dimensions previously detailed in the simulated results. In addition to the filter structures, two transitions were constructed and etched on the same substrate (RO3003), which allows the connection from the filter terminals to a Vector Network Analyzer (VNA) for its measurement. At the end of each transition, a 50 Southwest 1092-04A-5 end-launch connector is used, and its effect is removed from the measurements by using a specific TRL calibration kit designed for this experiment [17].

Fig. 9 contains the measurement results of the transmission and reflection coefficient of each constructed filter as a function of the frequency, and compared to the obtained simulation results. We can see that for the three constructed topologies, there is a good agreement on both coefficients when compared to the simulation results, with slight variations that can be mainly due to fabrication tolerances of the etching process and the produced gap between the top lid and the filter section. However, the measurement results confirm that all three structures, considering their measured performances, can be used for mm-wave communication technologies.

If we need to analyse which one of the topologies shows a better performance compared to simulations, the splitring resonator filter is the one with less difference in behaviour with respect to the simulation results and the other two topologies exhibit similar performance. Finally and in order to establish a comparison with other filter technologies in terms of the filter order, insertion losses (IL) and fractional bandwidth (FBW), a substrate integrated waveguide (SIW) [19], a multilayer low-temperature co-fired ceramic (LTCC) [20] and three different microstrip (MS) filters [21, 22, 23] operating in the Ka-band are compared with the implemented filters of this work, and shown in Table 1. From the compared technologies, we can see that SIW and IM-GWG have the lowest insertion losses values, being in line with previous studies [24], while the microstrip structures have the higher insertion losses when compared to the other implementations. Therefore, we can see that the proposed filters have lower insertion losses that other implementation done in standard microstrip technology, and comparable insertion losses with other published works, such as SIW, providing a suitable option for circuit designers for this frequency band. The performance of the filters in other aspects such as the roll-off, the rejection band or the bandwidth will be similar to equivalent designs implemented in microstrip technology with the advantage of the reduced insertion losses.
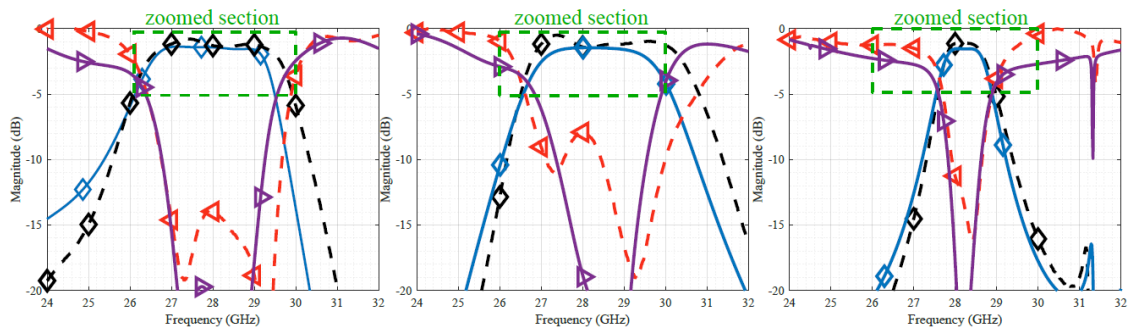
Figure 9: Measured transmission and reflection coefficient of each constructed filter as a function of the frequency,compared to the obtained simulation results. Left: parallel-coupled lines filter. Middle: end-coupled lines filter. Right: split-ring resonator filter.

5. Conclusions

This work presents the use of inverted microstrip gap waveguide for the design and construction of three different bandpass filters that are commonly used for communication systems. The designed filters show the advantage that have better performance in terms of transmission and reflection coefficient over the assessed band when compared with a standard inverted microstrip technology equivalent topology. In addition, the designed and constructed filters have the advantage that due to the low relative permittivity value of the section in which the field propagates, the dimensions of the etched lines tend to be larger in order to obtain the same impedances when using a standard microstrip topology.

This aspect can be a big decision factor when implementing this kind of filters, due to the overall cost that implies a very high-precision etching into a substrate.

An analysis of the tolerances of the three studied filter topologies w.r.t. the relative position of the lines and the pins below them shows that the filter made with split ring resonators is more robust to this uncertainty in this relative position. In addition, in the experimental results, this same topology is the one that exhibits the best agreement between simulated and measured results, which in summary means that is more robust to tolerances in general.

References

[1] 3GPP. Release description; Release 15. Technical specification (ts), 3rd Generation Partnership Project (3GPP), 03 2019. TR 21.915.

[2] T. S. Rappaport, S. Sun, R. Mayzus, H. Zhao, Y. Azar, K. Wang, G. N. Wong, J. K. Schulz, M. Samimi, and F. Gutierrez. Millimeter wave
mobile communications for 5G cellular: It will work! *IEEE Access*, 1:335–349, 2013. ISSN 2169-3536. doi: 10.1109/ACCESS.2013.
2260813.

[3] J.-S. Hong and M. J. Lancaster. *Microstrip Filters for RF/Microwave Applications*. John Wiley and Sons, Ltd, 2001. ISBN 9780471221616.

[4] E. Pucci, A. U. Zaman, E. Rajo-Iglesias, P. S. Kildal, and A. Kishk. Study of Q-factors of ridge and groove gap waveguide resonators. *IET
Microwaves, Antennas Propagation*, 7(11):900–908, August 2013. ISSN 1751-8725. doi: 10.1049/iet-map.2013.0081.

[5] Francisco Pizarro, David Ramirez-Gil, Astrid Algaba-Brazalez, Luis Fernando Herran-Ontanon, and Eva Rajo-Iglesias. Comparison study of
4x4 Butler matrices in microstrip technologies for Ka-band. *AEU - International Journal of Electronics and Communications*, 122:153248,
2020.

[6] A. Valero-Nogueira, M. Baquero, J. I. Herranz, J. Domenech, E. Alfonso, and A. Vila. Gap waveguides using a suspended strip on a bed of
nails. *IEEE Antennas and Wireless Propagation Letters*, 10:1006–1009, 2011.

[7] A. Vosoogh, A. A. Brazález, and P. Kildal. A V-band inverted microstrip gap waveguide end-coupled bandpass filter. *IEEE Microwave and
Wireless Components Letters*, 26(4):261–263, 2016. doi: 10.1109/LMWC.2016.2538598.

[8] E. Pucci, E. Rajo-Iglesias, and P. Kildal. New microstrip gap waveguide on mushroom-type EBG for packaging of microwave components.
IEEE Microwave and Wireless Components Letters, 22(3):129–131, 2012. doi: 10.1109/LMWC.2011.2182638.

[9] E. Pucci, E. Rajo-Iglesias, J. Vázquez-Roy, and P. Kildal. Planar dual-mode horn array with corporate-feed network in inverted microstrip gap
waveguide. *IEEE Transactions on Antennas and Propagation*, 62(7):3534–3542, 2014. doi: 10.1109/TAP.2014.2317496.

[10] C. Sanchez-Cabello, L. F. Herran, and E. Rajo-Iglesias. Ka-band diplexer for 5G mmwave applications in inverted microstrip gap waveguide
technology. *Electronics*, December 2020.

[11] J. Liu, A. Vosoogh, A. U. Zaman, and J. Yang. Design and fabrication of a high-gain 60-GHz cavity-backed slot antenna array fed by inverted
microstrip gap waveguide. *IEEE Transactions on Antennas and Propagation*, 65(4):2117–2122, 2017. doi: 10.1109/TAP.2017.2670509.

[12] A. Algaba-Brazalez, A. U. Zaman, and P. Kildal. Improved microstrip filters using pmc packaging by lid of nails. *IEEE Transactions on
Components, Packaging and Manufacturing Technology*, 2(7):1075–1084, 2012. doi: 10.1109/TCPMT.2012.2190931.

[13] T. S. Rappaport, S. Sun, R. Mayzus, H. Zhao, Y. Azar, K. Wang, G. N. Wong, J. K. Schulz, M. Samimi, and F. Gutierrez. Millimeter wave
mobile communications for 5G cellular: It will work! *IEEE Access*, 1:335–349, 2013. doi: 10.1109/ACCESS.2013.2260813.

[14] P. Kildal, E. Alfonso, A. Valero-Nogueira, and E. Rajo-Iglesias. Local metamaterial-based waveguides in gaps between parallel metal plates.
IEEE Antennas and Wireless Propagation Letters, 8:84–87, 2009. doi: 10.1109/LAWP.2008.2011147.

[15] E. Rajo-Iglesias and P. . Kildal. Numerical studies of bandwidth of parallel-plate cut-off realised by a bed of nails, corrugations and mushroomtype
electromagnetic bandgap for use in gap waveguides. *IET Microwaves, Antennas Propagation*, 5(3):282–289, 2011. doi: 10.1049/iet-map.
2010.0073.

[16] Nafsika Memeletzoglou, Carlos Sanchez-Cabello, Francisco Pizarro-Torres, and Eva Rajo-Iglesias. Analysis of periodic structures made of
pins inside a parallel plate waveguide. *Symmetry*, 11(4), 2019.

[17] Francisco Pizarro, Carlos Sánchez-Cabello, Jose-Luis Vazquez-Roy, and Eva Rajo-Iglesias. Considerations of impedance sensitivity and
losses in designing inverted microstrip gap waveguides. *AEU - International Journal of Electronics and Communications*, 124:153353, 2020.

[18] ANSYS website. https://www.ansys.com. Accessed on: 2020-10-09.

Evaluation of Inverted Microstrip Gap Waveguide Bandpass Filters for Ka-band

[19] F. Parment, A. Ghiotto, T. . Vuong, J. . Duchamp, and K. Wu. Ka-band compact and high-performance bandpass filter based on multilayer
air-filled SIW. *Electronics Letters*, 53(7):486–488, 2017.

[20] B. G. Choi, M. G. Stubbs, and C. S. Park. A ka-band narrow bandpass filter using ltcc technology. *IEEE Microwave and Wireless Components
Letters*, 13(9):388–389, 2003. doi: 10.1109/LMWC.2003.817139.

[21] H. Jiang, B. Lacroix, K. Choi, Y. Wang, A. T. Hunt, and J. Papapolymerou. *ka* - and *u* -band tunable bandpass filters using ferroelectric
capacitors. *IEEE Transactions on Microwave Theory and Techniques*, 59(12):3068–3075, 2011. doi: 10.1109/TMTT.2011.2170088.

[22] W. Zhao, Y. Zhang, and Y. Guo. A novel ka-band bandpass filter using microstrip closed loop resonators. In *2009 Asia Pacific Microwave
Conference*, pages 1443–1445, 2009. doi: 10.1109/APMC.2009.5384492.

[23] Y. Yan, Y. Chang, H. Wang, R. Wu, and C. H. Chen. Highly selective microstrip bandpass filters in ka-band. In *2002 32nd European
Microwave Conference*, pages 1–4, 2002. doi: 10.1109/EUMA.2002.339203.

[24] E. Rajo-Iglesias, M. Ferrando-Rocher, and A. U. Zaman. Gap waveguide technology for millimeter-wave antenna systems. *IEEE Communications
Magazine*, 56(7):14–20, 2018. doi: 10.1109/MCOM.2018.1700998.